Supplemental materials for "Impacts of transported background pollutants on summertime Western US air quality: model evaluation, sensitivity analysis and data assimilation", by Huang et al.

This file includes two tables and four figures.

Table A1. Wildfire plumes characteristics from the Multi-angle Imaging SpectroRadiometer (MISR) plume height project [a]

Region	Year	Number of plumes w/ power estimates	Total radiative of power (MW)	Median value of plume top heights (m ASL)	Radiative power/plume (MW)
Siberia	2002	541	269422	1367	498.01
	2003	985	474288	2225	481.51
	2006	433	148157	1597	342.16
	2008	1451	574766	1652	396.12
Canada (end of May to end of July)	2008	72	92439	2062	1283.9
NA	2002	445	371717	1815	835.32
	2004	1137	501585	1743	441.15
	2005	912	376329	1415	412.64
	2006	439	253488	2191	577.42
	2007	510	237497	1620	465.68

[a] Adapted from: http://misr.jpl.nasa.gov/getData/accessData/MisrMinxPlumes/

Table A2. US Geological Survey (USGS) land type numbers and descriptions [a]

Land type number	Land type description	Category used in Figure 3
1	Urban and Built-up Land	/
2	Dryland Cropland and Pasture	Cropland
3	Irrigated Cropland and Pasture	
4	Mixed Dryland/Irrigated Cropland and Pasture	
5	Cropland/Grassland Mosaic	
6	Cropland/Woodland Mosaic	
7	Grassland	Grass + Shrub
8	Shrubland	
9	Mixed Shrubland/Grassland	
10	Savanna	
11	Deciduous Broadleaf Forest	Forest
12	Deciduous Needleleaf Forest	
13	Evergreen Broadleaf	
14	Evergreen Needleleaf	
15	Mixed Forest	
16	Water Bodies	/
17	Herbaceous Wetland	/
18	Wooden Wetland	/
19	Barren or Sparsely Vegetated	/
20	Herbaceous Tundra	/
21	Wooded Tundra	/
22	Mixed Tundra	/
23	Bare Ground Tundra	/
24	Snow or Ice	/

[a] Adapted from: http://www.mmm.ucar.edu/wrf/users/docs/user_guide_V3/users_guide_chap3.htm#_Land_Use_and

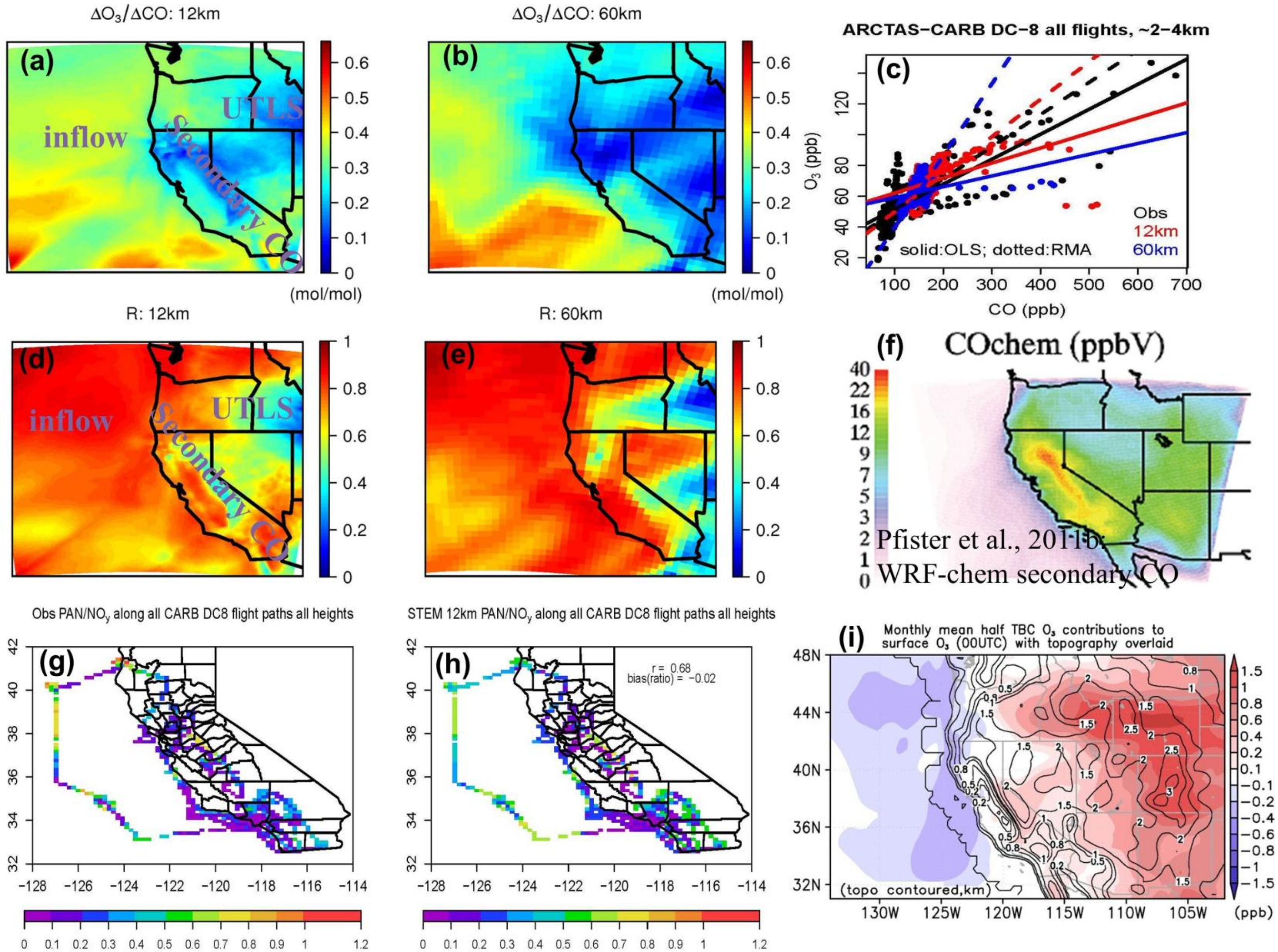

Figure A1. (a-b) Slope and (d-e) correlation of O_3 vs. CO at ~2.5 km AGL from (a;d) 12 km/32 layer and (b;e) 60 km/18 layer STEM base case for the studied period; (c) Scatterplot of O_3 vs. CO along all ARCTAS-CARB DC-8 flight paths (at ~2-4 km); (f) WRF-chem tracer predicted secondary CO during the same study period in Pfister et al. (2011b); (g) Observed and (h) STEM 12 km modeled PAN/NO_y along all ARCTAS-CARB DC-8 flights at all altitudes; (i) Period mean 00 UTC surface O_3 sensitivity to half reduction in TBC O_3.

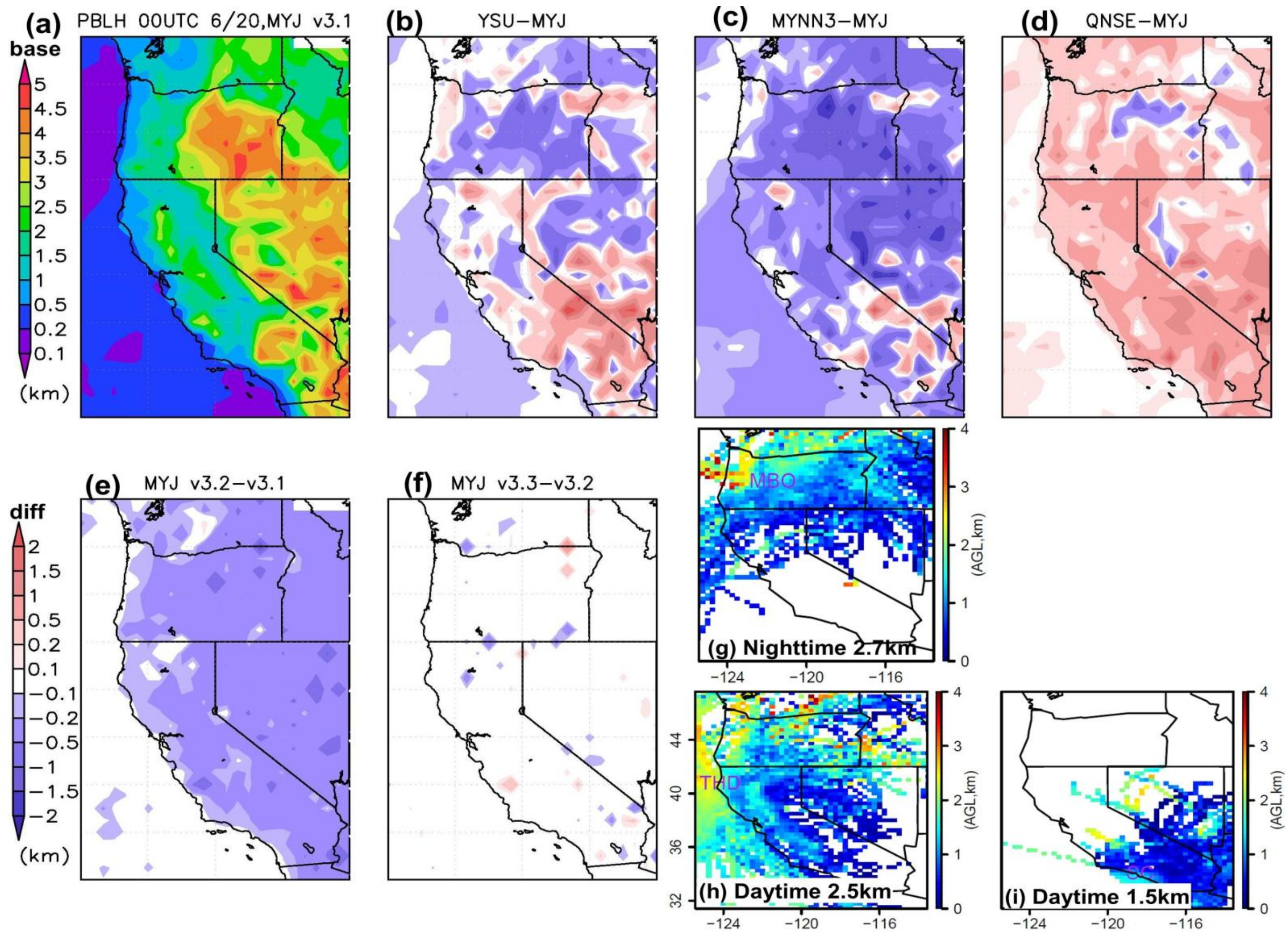

Figure A2. (a) 12 km WRF (Version 3.1)-predicted PBLH at 00 UTC, 20 June, by using the MYJ PBL scheme; Differences of WRF-predicted PBLH between the cases using (b) YSU; (c) MYNN3; and (d) QNSE PBL schemes and the results in (a); Differences of predicted PBLH between the cases using (e) WRF Version 3.2 and (f) WRF Version 3.3 and the results in (a); Similar as findings by Saide et al. (2011) over Santiago, Chile, overall MYNN3 and QNSE schemes generate the shallowest and deepest PBLH, respectively, and the differences between YSU and MYJ schemes vary by region. (g) PDT 9pm-7am forward trajectories (calculated mean transport altitudes in km, AGL for every 0.25 degree) during the study period originating from MBO 2.7 km ASL; PDT 8am-8pm forward trajectories during the studied period originating from (h) THD 2.5 km ASL and (i) SC 1.5 km ASL.

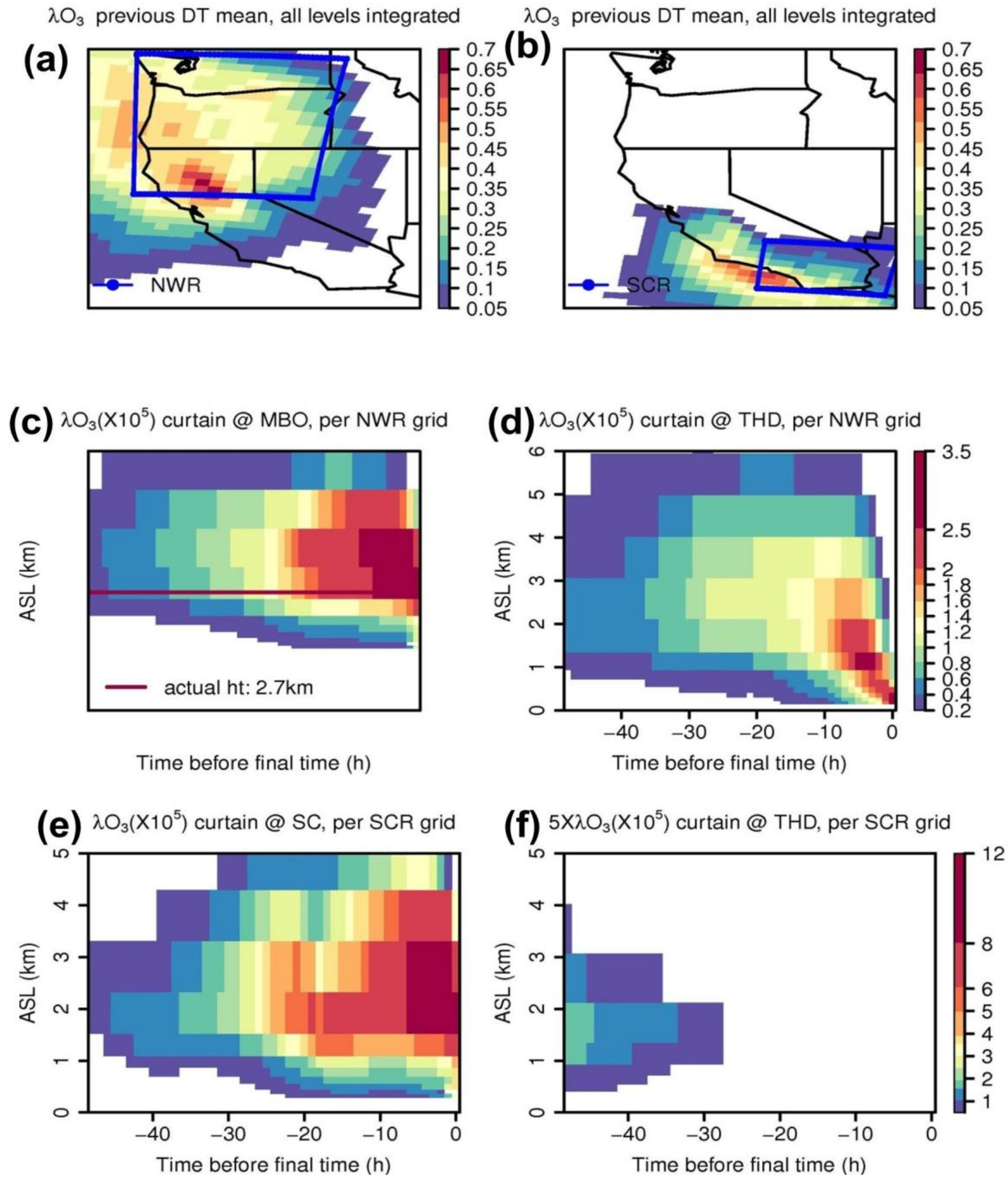

Figure A3. Same as Figure 9 but for results from the 60 km/18 layer grid.

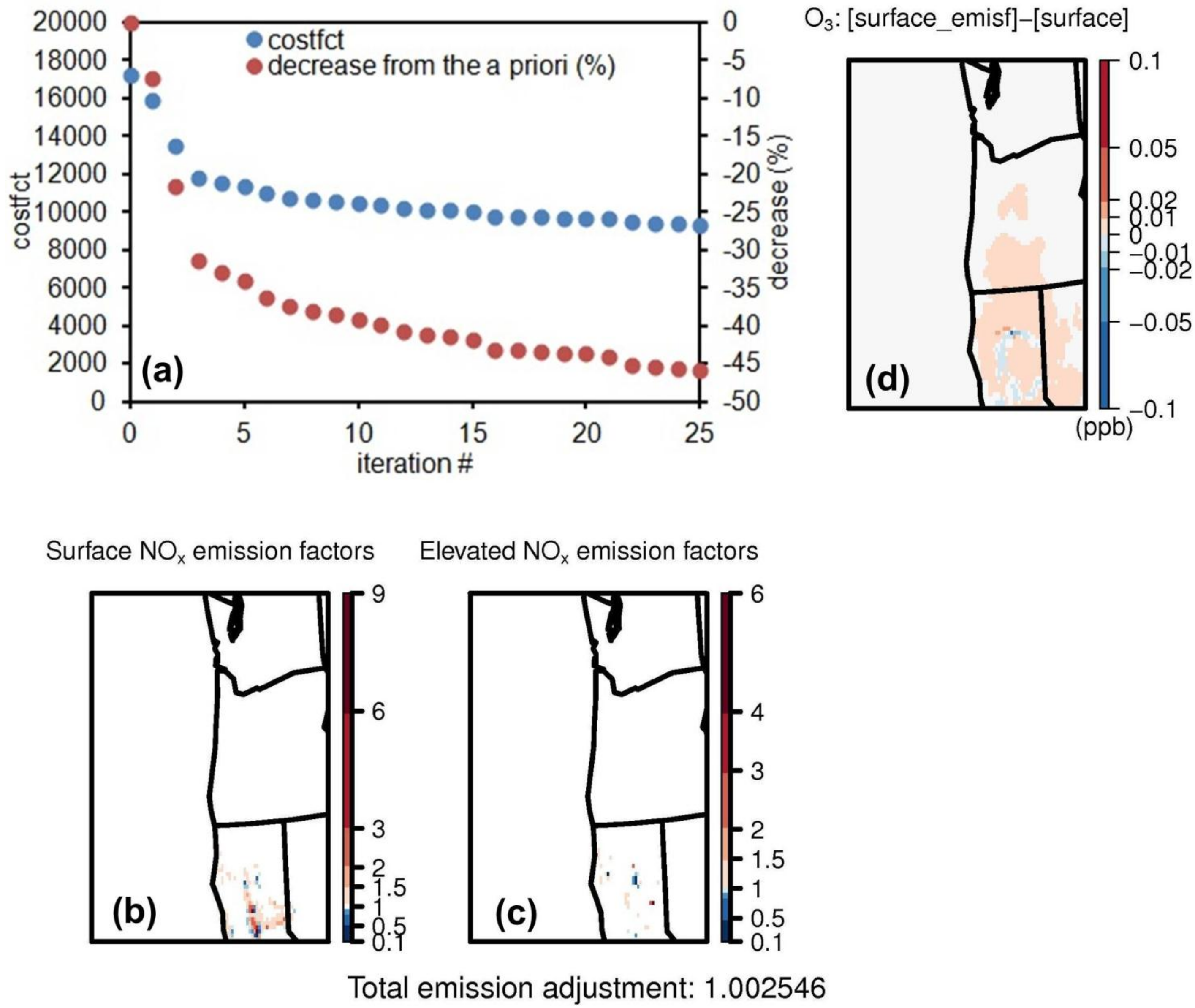

Figure A4. (a) Cost function and its reduction as a function of iteration number in Case AS; (b) Surface and (c) elevated NO_x emission scaling factors by controlling NO_x emissions and assimilating surface NO_2 observations in a 24-hour window; (d) Daytime mean surface O_3 differences: assimilating surface observation while applying NO_x emission scaling factors-Case AS.